DALTON
FULL PAPER

Resonance Raman spectroelectrochemical and structural study of reduced ruthenium(II) complexes with binaphthyridine-based ligands

Sonya M. Scott,[a] Anthony K. Burrell,*[b] Paul A. Cocks[a] and Keith C. Gordon*[a]

[a] *Department of Chemistry, University of Otago, PO Box 56, Dunedin, New Zealand.*
E-mail: kgordon@alkali.otago.ac.nz
[b] *Institute of Fundamental Science-Chemistry, Massey University, Private Bag 11122,*
Palmerston North, New Zealand

Received 17th August 1998, Accepted 4th September 1998

The spectroscopy of electrochemically reduced ruthenium(II) complexes with 2,2′-biquinoline and 2,2′-binaphthyridine ligands have been investigated. These compounds are: $[Ru(bn)(bpy)_2][BF_4]_2$ (where bn = 2,2′-bi-1,8-naphthyridine and bpy = 2,2′-bipyridyl); $[Ru(dbn)(bpy)_2][BF_4]_2$ (where dbn = 3,3′-dimethylene-2,2′-bi-1,8-naphthyridine); $[Ru(dbn)_3][BF_4]_2$; $[Ru(dbq)(bpy)_2][BF_4]_2$ (where dbq = 3,3′-dimethylene-2,2′-biquinoline). Resonance Raman spectra of the parent species showed the bichromophoric nature of the visible absorptions of the heteroleptic complexes; both bpy and non-bpy ligand vibrations are enhanced depending on the excitation wavelength. Changes in the electronic absorption spectra for the complexes upon electrochemical reduction suggest the reducing electron is localised on the non-bpy ligand. For the complexes with the dimethylenebinaphthyridine ligand the second reduction also appears localised on the non-bpy ligand. Resonance Raman spectra of the reduced species confirm that the first and second reduction are based on the dbn ligand. Single crystal structures of $[Ru(bn)(bpy)_2][BF_4]_2$ and $[Ru(dbn)(bpy)_2][BF_4]_2$ have been determined and significant distortions of the ligands are apparent.

Introduction

Ruthenium(II) complexes with 2,2′-biquinoline or binaphthyridine ligands are of interest because of their electrochemical and electronic properties.[1] These complexes have low energy metal-to-ligand charge-transfer (MLCT) excited states and have potential uses in solar energy and photocatalytic systems.[2]

Our interest in these complexes derives from the ease of reduction of the binaphthyridine ligands. Such ligands ensure that photoexcitation of the complex results in the formation of a radical anion on the binaphthyridine ligand as part of the MLCT excited state. However, if the ligands are readily reduced it may be possible to produce a doubly reduced ligand anion. A multiply reduced ligand could act as a potent reducing agent in a multielectron transfer sense. If this could be achieved through photoexcitation then the possibility of multielectron photocatalysis may be realisable through this strategy. However, for such a strategy to succeed it is necessary to establish that both the first and second reductions of these complexes are localised on the bn or dbn ligands. The compounds are: $[Ru(bn)(bpy)_2][BF_4]_2$ **1** (where bn = 2,2′-bi-1,8-naphthyridine and bpy = 2,2′-bipyridyl); $[Ru(dbn)(bpy)_2][BF_4]_2$ **2** (where dbn = 3,3′-dimethylene-2,2′-bi-1,8-naphthyridine); $[Ru(dbn)_3][BF_4]_2$ **3**; $[Ru(dbq)(bpy)_2][BF_4]_2$ **4** (where dbq = 3,3′-dimethylene-2,2′-biquinoline). The ability of the ligand to store charge may also be mediated by the degree of planarity of the ligand. We report in this paper how a series of complexes behave when reduced in terms of their spectroscopic properties. We show that the first and second reductions for complex **2** are localised on the dbn ligand.

Experimental

Ligand synthesis

Ligands were prepared following Thummel *et al.*[3] and Uhlemann *et al.*[4] All were hygroscopic as previously noted.

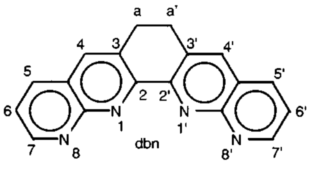

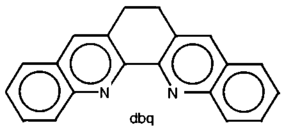

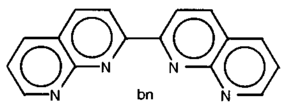

Complex synthesis

The complex $[Ru(bpy)_2Cl_2]\cdot 2H_2O$ was synthesized from $RuCl_3\cdot H_2O$ using the method of Togano *et al.*[5] The $[RuL(bpy)_2]^{2+}$ complexes were prepared following the literature procedure of Strekas and co-workers[6] by refluxing one equivalent of $[Ru(bpy)_2Cl_2]\cdot 2H_2O$ with one equivalent of ligand in ethanol for 48 h. The complex was precipitated by addition of NH_4BF_4 in water. Complexes were crystallised from dichloromethane by diethyl ether diffusion and their purity was confirmed by microanalysis.

Physical measurements

A Perkin-Elmer Lambda-19 spectrophotometer was used for collection of electronic absorption spectra. This was calibrated with a Ho_2O_3 filter and spectra were run with a 2 nm resolution.

The experimental apparatus for measurement of Raman spectra has been described previously;[7] briefly, Raman scattering was generated using continuous wave (Spectra-Physics Model 166 argon ion laser). The sample was held in a spinning NMR tube, or optically transparent thin-layer electrode (OTTLE) cell. Spectra were calibrated using emission lines from a neon lamp or from an argon ion laser. The calibrations were checked by measuring the Raman band wavenumber positions for a known solvent.[8] It was found that, for the data reported herein, the calibrations were accurate to *ca.* 1 cm^{-1}. A 150 µm slit width was used on the spectrograph and this gave a resolution of *ca.* 6 cm^{-1} with 457.9 nm excitation.

The electronic absorption spectra of reduced species were measured using an OTTLE cell with a platinum grid as the working electrode.[9] The potential applied was stepped through the redox processes, collecting a spectrum at each step. For Raman spectra of reduced species a similar cell was employed. In these experiments the potential applied was sufficient to ensure complete reduction of the sample in the irradiated volume. The potential applied was *ca.* 0.4 V greater than the $E°$ value due to the *IR* drop across the cell.[10] This was determined from a study of metal carbonyl complexes in which reduction results in complete bleaching of a parent species band thus permitting calibration of the OTTLE cell characteristics.† In the case of complex **2**, for which two distinct reduced species spectra are observed, the first spectrum was generated by application of a reducing potential of *ca.* −1.2 V *vs.* silver wire, the second by application of a potential of −1.6 V.

Initial measurements found that the signal-to-noise ratios of the Raman spectra were reduced because of reflection off the platinum grid. This problem was alleviated by removing a portion of the centre of the grid (*ca.* 2 × 4 mm) and aligning the laser to irradiate the solution in that region.

Crystallography

Single crystals of complexes $\mathbf{1}\cdot CH_2Cl_2$ and $\mathbf{2}\cdot CH_2Cl_2$ were grown by the slow diffusion of diethyl ether into a solution of **1** or **2**, respectively, dissolved in dichloromethane. Purple rod shaped crystals with approximate dimensions 0.58 × 0.4 × 0.4 and *ca.* 0.2 × 0.43 × 0.2 mm respectively were secured to the end of a glass fibre with cyanoacrylate glue and cooled to −100 °C in a nitrogen stream. Data collection, reduction,[12] solution and refinement[13] were performed as previously described.[11]

Crystal data. *For* $\mathit{1}\cdot CH_2Cl_2$. $C_{37}H_{28}B_2Cl_2F_8N_8Ru$, $M = 930.26$, monoclinic, space group $P2_1/c$, $a = 13.437(3)$, $b = 12.804(3)$, $c = 21.869(4)$ Å, $\beta = 102.18(3)°$, $U = 3675(1)$ Å^3, $T = 173$ K, $Z = 4$, μ(Mo-Kα) = 0.655 mm^{-1}, 3597 reflections measured, 3407 unique ($R_{int} = 0.0815$) which were used in all calculations. The final $Rw(F_o^2) = 0.1115$ [$R(F_o) = 0.0392$], where $w^{-1} = \sigma^2(F_o^2) + (aP)^2 + bP$ and $a = 0.1022$, $b = 7.09$ and $P = [\max(F_o^2,0) + 2F_c^2]/3$. The structure was refined on F_o^2 using all data; the value in parentheses is given for comparison with older refinements based on F_o with a threshold of $F > 4\sigma(F)$; *R* factors based on F^2 are statistically about twice as large as those based on *F*.

For $\mathit{2}\cdot CH_2Cl_2$. $C_{39}H_{30}B_2Cl_2F_8N_8Ru$, $M = 956.3$, monoclinic, space group $P2_1/c$, $a = 13.387(3)$, $b = 13.020(3)$, $c = 22.213(4)$ Å, $\beta = 101.01(3)°$, $U = 3800(2)$ Å^3, $T = 173$ K, $Z = 4$, μ(Mo-Kα) = 0.636 mm^{-1}, 6956 reflections measured, 6648 unique ($R_{int} = 0.0716$) which were used in all calculations. The final $Rw(F_o^2) = 0.0971$ [$R(F_o) = 0.0421$], where $w^{-1} = \sigma^2(F_o^2) + (aP)^2 + bP$ and $a = 0.0502$, $b = 1.65$ and $P = [\max(F_o^2,0) + 2F_c^2]/3$. Other details as above.

Selected bond lengths and angles are given in Table 1.

CCDC reference number 186/1150.

Results and discussion

Crystallography

The molecular structure of the cationic portion of complex $\mathbf{1}\cdot CH_2Cl_2$ is shown in Fig. 1. The ruthenium atom is held in a distorted octahedral environment. There are significant differences in the Ru–N bond lengths between the bpy ligands and those of the bn ligand. The Ru–N bond lengths for the bpy ligands are in the range 2.047(4)–2.058(4) Å. The Ru–N distances for the bn ligand are 2.102(4) (N2) and 2.089(4) Å (N3). This difference is attributed to the more sterically demanding nature of the bn ligand. The bulky nature of the bn ligand has a strong influence on the structure of the complex as a whole. The bpy ligands demonstrate two different responses to the steric pressure applied by the bn ligand. One of the bpy ligands (rings G and H) twists slightly to minimise the interactions and has a torsion angle between the two pyridyl rings (G and H) of 4.8(9)°. It also adopts a configuration where the planes between the two pyridyl rings (G and H) are at 8.3(4)°, being bent about a point between the two rings. The second bpy ligand (rings E and F) deals with the steric pressure by twisting to a much greater extent, with a torsion angle between the two rings (E and F) of 11.8(9)°. The angle between the two ring planes (E and F) is 12.1(4)°. The steric pressure about this ruthenium centre is also evident in the deformations observed on the bn ligand.

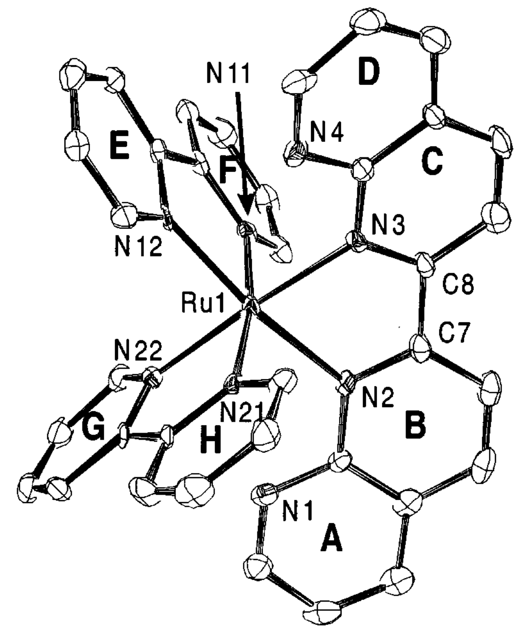

Fig. 1 An ORTEP[14] drawing of complex **1**. Thermal ellipsoids are shown at 30% probability.

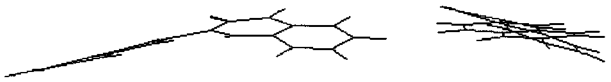

Fig. 2 Line drawing showing the geometry of the bn ligand in complex **1**.

Only one other structure containing a co-ordinated bn ligand is known.[15] The bn ligand in $[Cu(bn)(PPh_3)_2]$ while distorted from planarity *via* a torsional twist did not display any of the deviations from planarity observed for complex **1** and the related 2,2′-biquinoline (biq) ligand.[16] One of the notable features associated with complexes of the biq ligand is a tendency for it to take on a banana shape. This distortion while absent in $[Cu(bn)(PPh_3)_2]$ is clearly present in **1**, and is shown in Fig. 2. The torsion angle between the two naphthyridines (rings A,B and rings C,D) is 11.4(8)° and the angle between the planes of the pyridyl rings of B and C is 16.8(3)°. Moreover, the angle between the planes of the most distant pyridyl rings (A and D) is 21.5(5)°. This banana shape is largely achieved at the expense of only one of the naphthyridine rings. The naphthyridine ring consisting of A and B is effectively planar with the angle

---

† The OTTLE cell used in these measurements has been tested on other complexes. These show that for a reduction occurring at −0.75 V *vs.* SCE a reducing potential of *ca.* −1.1 V *vs.* silver wire is required in the OTTLE cell to ensure no residual parent species is observed.[11]

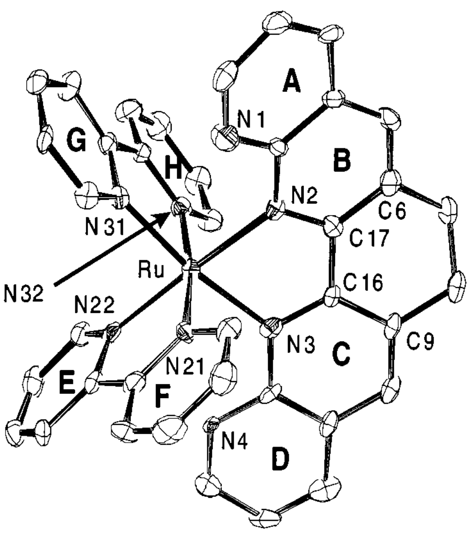

Fig. 3 An ORTEP drawing of complex **2**. Thermal ellipsoids are shown at 30% probability.

between the two pyridyl planes being 0.7(3)°. In contrast the other naphthyridine ring is significantly bent. The angle between the planes of the pyridyl rings (C and D) is 5.5(2)°. The dichloromethane of crystallisation and the BF_4^- counter ions do not interact with the cationic portion of the molecule in any fashion and there are no intermolecular interactions between cations.

The molecular structure of the cationic portion of complex **2**·CH_2Cl_2 is shown in Fig. 3. Many of the same structural elements described for **1** are also present in **2**. The ruthenium atom is held in a distorted octahedral environment. The differences in the Ru–N bond lengths between the bpy ligands and the dbn ligand are not as pronounced as in **1** but are still present. The Ru–N bond lengths for the bpy ligands are in the range 2.047(5)–2.056(5) Å, those for the dbn ligand are 2.086(5) (N2) and 2.095(5) Å (N3). As with bn the bulky nature of the dbn ligand has a strong influence on the structure of the complex. The bpy ligands demonstrate the same two different responses to the steric pressure as observed in **1**. One of the bpy ligands (rings E and F) twists slightly to minimise the interactions and has a torsion angle between the two pyridyl rings of 3.7(9)°. It also adopts a configuration where the angle between the planes of the two pyridyl rings (E and F) is 9.0(4)°, bending about a point between the rings. The result is a bowing of the bpy ligand. The second bpy ligand (G and H) deals with the steric pressure by twisting to a much greater extent, with a torsion angle between the two rings (G and H) of 11.0(9)°. The angle between the two planes, of G and H, is considerably less in this instance at 8.1(3)°.

The steric pressure about this ruthenium centre is also evident in the deformations observed on the dbn ligand. Several complexes incorporating the dbn ligand have been reported.[17] In most cases the only significant distortion of the dbn ligand results from the expected torsional twist of the 2,2′ bond. However, in **2**, $Ru(dbn)_3^{2+}$ and $Ru(dbn)_3^{+}$ much more significant distortions are apparent.[17c]

The torsion angle between the two naphthyridines (rings A,B and C,D) is in the range expected at 15.4(8)°. However the angle between the planes of the pyridyl rings of B and C is 17.4(3)°, with that between the planes of A and D being 25.0(2)°. As with the bn ligand on **1** this results in a banana shape, shown for dbn in Fig. 4, and is achieved at the expense of one of the naphthyridine rings. The naphthyridine ring consisting of C and D is effectively planar with the angle between the two pyridyl planes being 1.0(3)°. In contrast the other naphthyridine ring (A,B) is significantly bent. The angle between the planes of the pyridyl rings (A and B) is 8.5(2)°. The dichloromethane of crystallisation and the BF_4^- counter ions do not interact with the cationic portion of the molecule in any fashion and there are no intermolecular interactions between cations.

Table 1 Selected bond lengths (Å) and angles (°)

1·CH_2Cl_2		**2**·CH_2Cl_2	
Ru(1)–N(22)	2.047(4)	Ru–N(22)	2.050(5)
Ru(1)–N(12)	2.054(4)	Ru–N(21)	2.047(5)
Ru(1)–N(21)	2.052(4)	Ru–N(31)	2.056(5)
Ru(1)–N(11)	2.058(4)	Ru–N(32)	2.054(5)
Ru(1)–N(3)	2.089(4)	Ru–N(2)	2.086(5)
Ru(1)–N(2)	2.102(4)	Ru–N(3)	2.095(5)
N(22)–Ru(1)–N(12)	86.8(2)	N(22)–Ru–N(21)	79.4(2)
N(22)–Ru(1)–N(21)	78.9(2)	N(22)–Ru–N(31)	87.9(2)
N(12)–Ru(1)–N(21)	94.4(2)	N(21)–Ru–N(31)	96.2(2)
N(22)–Ru(1)–N(11)	94.2(2)	N(22)–Ru–N(32)	94.6(2)
N(12)–Ru(1)–N(11)	79.1(2)	N(21)–Ru–N(32)	172.2(2)
N(21)–Ru(1)–N(11)	170.9(2)	N(31)–Ru–N(32)	78.5(2)
N(22)–Ru(1)–N(3)	176.3(2)	N(22)–Ru–N(2)	176.5(2)
N(12)–Ru(1)–N(3)	96.5(2)	N(21)–Ru–N(2)	98.1(2)
N(21)–Ru(1)–N(3)	99.2(2)	N(31)–Ru–N(2)	94.8(2)
N(11)–Ru(1)–N(3)	88.0(2)	N(32)–Ru–N(2)	88.2(2)
N(22)–Ru(1)–N(2)	99.3(2)	N(22)–Ru–N(3)	99.3(2)
N(12)–Ru(1)–N(2)	171.9(2)	N(21)–Ru–N(3)	90.9(2)
N(21)–Ru(1)–N(2)	92.0(2)	N(31)–Ru–N(3)	170.7(2)
N(11)–Ru(1)–N(2)	95.1(2)	N(32)–Ru–N(3)	95.0(2)
N(3)–Ru(1)–N(2)	77.5(2)	N(2)–Ru–N(3)	78.2(2)

Fig. 4 Line drawing showing the geometry of the dbn ligand in complex **2**.

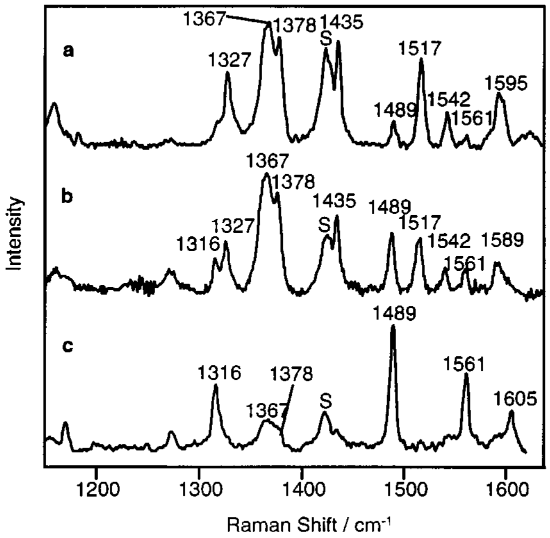

Fig. 5 Resonance Raman spectra of complex **1** in CH_2Cl_2: (a) excitation wavelength = 514.5 nm, 30 mW; (b) excitation wavelength = 488 nm, 30 mW; (c) excitation wavelength = 457.9 nm, 20 mW; S denotes solvent bands.

Spectroscopy

The resonance Raman spectra of complex **1** as a function of excitation wavelength are shown in Fig. 5. The frequencies of the observed bands for the complexes are listed in Table 2 along with their assignments.

The resonance Raman spectra of the heteroleptic complexes **1**, **2** and **4** show the bichromophoric nature of these complexes. At Raman excitation wavelengths to the blue (457.9 nm),

Table 2 Observed Raman bands (cm^{-1}) for complexes

	1		**2**		**3**		**4**	
λ_{exc}/nm	457.9	514.5	457.9	514.5	457.9	514.5	457.9	514.5
	1605[a]		1604[a]	1600	1605w[b]	1605w[b]	1605s[a]	1605[a]
		1595[c]						1597[d]
	1561s[a]	1561w[a]	1562s[a]		1556w[b]	1556w[b]	1554s[a]	1554[a]
		1542[c]		1543w[b]				
		1517s[c]						
	1489s[a]	1489w[a]	1490s[a]	1495w[a]	1491[b]	1500[b]	1487s[a]	1487w[a]
		1435s[c]		1431s[b]		1444[b]	1460w[d]	1460s[d]
	1378w[c]	1378s[c]	1374[b]	1374[b]		1435[b]		1433w[d]
	1367w[c]	1367s[c]			1372[b]	1372[b]		1357[d]
		1327[c]						
	1316[a]		1317[a]				1317s[a]	1317[a]

s = Strong; w = weak. [a] bpy modes. [b] dbn modes. [c] bn modes. [d] dbq modes.

Table 3 Electronic absorption data for complexes (CH_2Cl_2 solution) and their reduced and oxidised products

Complex	λ/nm ($\varepsilon \times 10^{-3}$/$M^{-1}$ cm^{-1})							
1	346 (37)		436 (11)		574 (9)			
2	369 (32)	394 (24)	440 (8)		576 (9)			
3	358 (56)	388 (33)		560 (8)	582 (10)			
4	373 (15)	395 (22)	440 (6)	528 (7)				
$\mathbf{1}^-$		343 (28)	373 (25)	413 (25)	503 (16)	624 (7)	829 (4)	941 (9)
$\mathbf{2}^-$	292 (63)	337 (23)	381 (26)	415 (30)	500 (13)	614 (6)	800 (5)	920 (11)
$\mathbf{3}^-$			362 (26)	417 (13)	630 (6)	719 (6)	817 (5)	
$\mathbf{2}^{2-}$	294 (53)		356 (31)	469 (18)	538 (15)	723 (15)	794 (13)	
$\mathbf{3}^{2-}$		362 (50)	387 (53)	443 (42)	723 (30)	785 (34)	862 (27)	

the modes enhanced are those of the bpy ligand. These are enhanced through the MLCT transition of Ru→bpy. The modes enhanced lie at *ca.* 1316, 1489, 1561 and 1605 cm^{-1} [Fig. 5(c)]. As the excitation wavelength is tuned to longer wavelengths the modes associated with the non-bpy ligand become enhanced. The resonance Raman spectra of homoleptic complex **3** show dbn modes only. They reveal that there are dbn based bands at 1491, 1556 and 1605 cm^{-1} which are near coincident with those of bpy. The modes observed in the spectra of complex **3** are very close in wavenumber to those of other complexes with this ligand, such as $Cu(dbn)_2^+$.[17b] The resonance Raman spectra of complexes **1** and **2** are alike as might be expected in view of their similar structures.

The changes in the electronic absorption spectra that occur upon electrochemical oxidation or reduction of the complexes are summarised in Table 3. Oxidation has two effects on the electronic absorption spectra of the complexes: first, the MLCT transitions in the visible are bleached. Secondly, the ligand based transitions at *ca.* 360 nm are red-shifted upon oxidation. These spectral changes are consistent with oxidation at the metal and support the assignment previously made by Thummel and Lefoulon[18] and the spectral changes observed in copper(I) complexes of these ligands.[17b]

The changes in the electronic absorption spectra of the complexes upon reduction are more interesting. Complexes **1** and **2** show the growth of a band at *ca.* 930 nm upon application of a potential more negative than that of their first reductions. Complex **3** also shows the growth of a band upon reduction, however, the absorption is centred at *ca.* 719 nm and the $\mathbf{3}^-$ species does not absorb strongly at 930 nm. The spectral similarity of $\mathbf{1}^-$ and $\mathbf{2}^-$ suggest the presence of similar species in each reduced complex. The spectral signatures observed are consistent with the formation of a $dbn^{\bullet -}$ species. These show absorptions at 950 and 1050 nm for electrochemically reduced copper(I) complexes.[15,17b] A recent paper describing the crystal structure of $\mathbf{3}^-$ by Echegoyen and co-workers[17c] suggested that the reducing electron was delocalised over two of the dbn ligands. Our OTTLE measurements suggest that $\mathbf{3}^-$ does not contain a $dbn^{\bullet -}$ species. It is possible that $\mathbf{3}^-$ in solution also has the delocalising properties observed in the solid state.

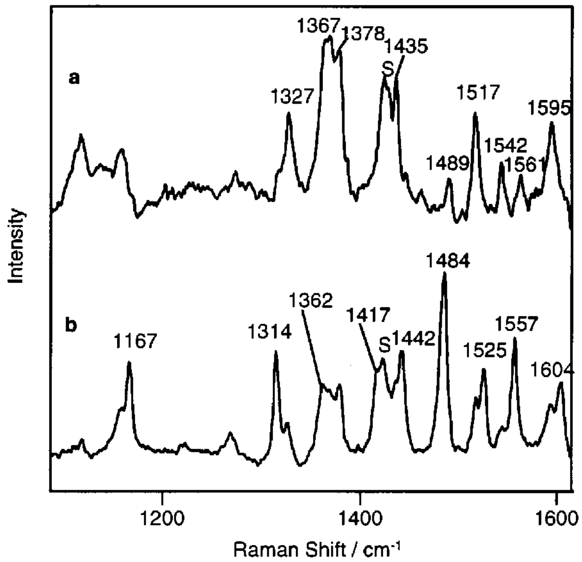

Fig. 6 Resonance Raman spectrum with 514.5 nm excitation (30 mW) of (a) **1** and (b) $\mathbf{1}^-$. Solvent (CH_2Cl_2) bands denoted by S.

On application of a more reducing potential to complex $\mathbf{1}^-$ no appreciable spectral changes are observed. The reduced complexes $\mathbf{2}^-$ and $\mathbf{3}^-$ may be further reduced, resulting in significant bandshifts for each spectrum. For $\mathbf{2}^- \longrightarrow \mathbf{2}^{2-}$ the 930 nm band is depleted in intensity with a new band growing in at 723 nm; similar behaviour is observed for $\mathbf{3}^- \longrightarrow \mathbf{3}^{2-}$.

The changes that occur in the resonance Raman spectra of complexes **1**–**3** as a function of reduction are presented in Figs. 6–8. In the case of **2** two distinct spectral signatures may be observed. For **1** and **3** application of a reducing potential more negative than each complex's first reduction potential results in distinct spectral changes. However, when even more negative

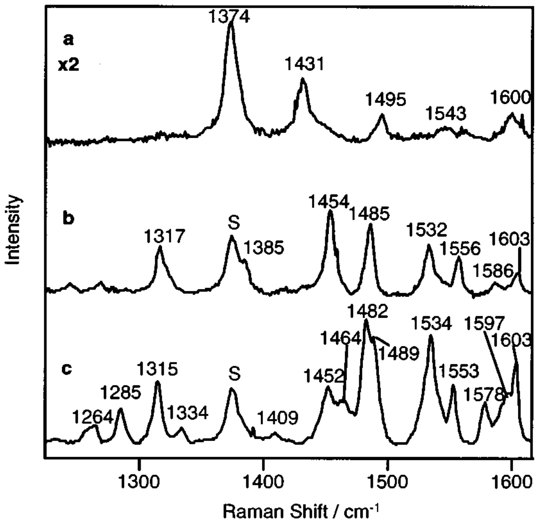

Fig. 7 Resonance Raman spectrum with 514.5 nm excitation (30 mW) of (a) **2**; (b) $\mathbf{2}^-$; (c) $\mathbf{2}^{2-}$. Solvent (CH_3CN) bands denoted by S.

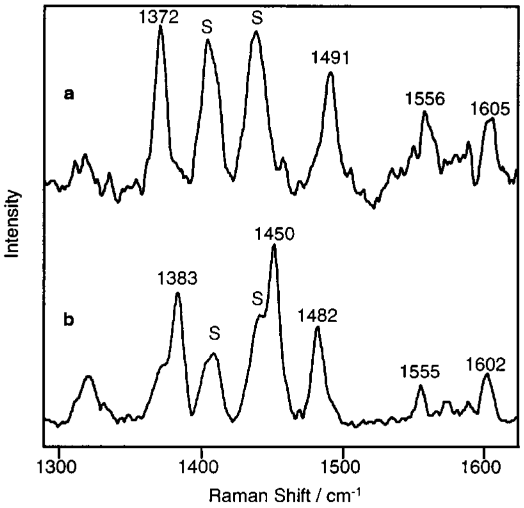

Fig. 8 Resonance Raman spectrum with 457.9 nm excitation (30 mW) of (a) **3** and (b) $\mathbf{3}^-$. Solvent (dmf) bands denoted by S.

potentials are applied, such that second reductions may occur, the Raman spectra become obscured by increased broad backgrounds. For all three complexes it is possible to reproduce the ground state spectrum upon reoxidation of the first reduction product. For **2** it is also possible to do this for the second reduction product. However **1** and **3** do not show this type of reversibility.

The resonance Raman spectrum of complex $\mathbf{3}^-$ with 457.9 nm excitation shows bands at 1450 and 1383 cm^{-1}; also of note are weak bands at 1372 and 1491 cm^{-1}. At the potential used in the OTTLE cell, complete conversion into $\mathbf{3}^-$ within the irradiated volume occurs.[11] Echegoyen and co-workers[17c] have found that in the solid state the $\mathbf{3}^-$ appears to have the reducing electron spread over two dbn ligands, thus having the formula: $[\mathrm{Ru}(\mathrm{dbn}^{-\frac{1}{2}})_2(\mathrm{dbn})]^+$. Most studies of $[\mathrm{Ru(L)}_3]^{2+}$ (where L is a bidentate polypyridyl ligand) indicate that upon electrochemical reduction species of the type $[\mathrm{Ru(L)}_2(\mathrm{L}^{\bullet-})]^+$ are formed.[19] The resonance Raman spectrum of $\mathbf{3}^-$ is ambiguous as to the nature of the reduced species; bands are observed at 1490 and 1602 cm^{-1} which may be due to $dbn^{\bullet-}$ features. However, these bands are only slightly shifted from those of the neutral dbn ligand; such a shift to lower wavenumber may occur because of the one electron reduction of a single dbn ligand, or the partial reduction of a number of the ligands.

The resonance Raman spectra of complexes $\mathbf{1}^-$ and $\mathbf{2}^-$ measured with 514.5 nm excitation show dramatic changes from the spectra of their parent species. Of note is the growth of a group of bands that appear to be associated with the bpy ligand. These lie at 1167, 1314, 1484, 1557 and 1604 cm^{-1} for $\mathbf{1}^-$ and at 1317, 1485, 1556 and 1603 cm^{-1} for $\mathbf{2}^-$. The pattern of intensities is remarkably similar to that observed in the resonance Raman spectra of **1** and **2** with 457.9 nm excitation (Fig. 5, trace c for **1**). Two points are worthy of note: first, the spectra at 514.5 nm show no bpy vibrations for the parent complexes **1** and **2**. Secondly, the frequencies of some of the bpy vibrations observed for complexes $\mathbf{1}^-$ and $\mathbf{2}^-$ are lower than those of the corresponding parent complexes. The bpy vibrations can be enhanced through the Ru→bpy MLCT chromophore; the wavelength of absorption of this chromophore may be shifted by reduction of a ligand bound to the metal.[20,21] This would explain why the bpy vibrations become strongly enhanced with 514.5 nm excitation when the complexes are reduced but are not observed for the parent species. The observation of a shift to lower frequency for a number of the bands may be explained in terms of a reduction at the bn or dbn ligand. The bpy vibrations are frequency sensitive to the oxidation state of the metal centre in $\mathrm{Ru(bpy)}_3{}^{2+}$. The corresponding ruthenium(III) complex shows a Raman spectrum in which the bpy vibrations shift up in wavenumber by about 6–7 cm^{-1}.[22] Hence any reduction in the electron density of the ruthenium(II) centre should result in a *lowering* of the bpy frequencies. This effect has been observed in a series of studies on the resonance Raman spectra of ruthenium(II) diimine complexes by Wertz and co-workers.[21] In the resonance Raman spectrum of $[\mathrm{Ru(dpbpy)}_3]^{2+}$ (dpbpy = 4,4′-diphenyl-2,2′-bipyridine) and the first and second reduced species the neutral ligand modes were observed to shift to lower frequencies. A rationale for this observation would be that the redox MO has a contribution from the metal d orbitals hence reduction of the ligand causes an increase in electron density at the metal and reduction in frequency for the bpy modes. Calculations on dbn and related ligands[23] reveal that the wavefunction amplitude of the π* MO, for the chelating N atoms, is greater for 2,2′-bipyridine than for dbn. Thus population of the π* MO by reduction at the ligand would perturb the electron density at the metal more if the reduction is at bpy than dbn. This increase in electron density at the metal with ligand reduction is well documented in metal carbonyl complexes as well as substituted bipyridyl systems.[24]

The remaining bands observed in the spectra of complexes $\mathbf{1}^-$ and $\mathbf{2}^-$ are assigned as $bn^{\bullet-}$ and $dbn^{\bullet-}$ modes respectively. These lie at 1442, 1525 and 1590 cm^{-1} for $\mathbf{1}^-$. The resonance Raman spectrum of $[\mathrm{Cu(bn)(PPh_3)_2}]^0$, in which the ligand is reduced, shows features at 1439, 1484 and 1592 cm^{-1}.[15] The spectrum of $\mathbf{1}^-$ shows a strong neutral bpy band at 1484 cm^{-1}. In the spectrum of $\mathbf{2}^-$, with 514.5 nm excitation, bands may be seen at 1385, 1454, 1532 and 1586 cm^{-1}. These correspond to the $dbn^{\bullet-}$ bands previously observed for $[\mathrm{Cu(dbn)(PPh_3)_2}]^0$, at 1396, 1447, 1485, 1540, 1570, 1586 and 1623 cm^{-1}.

It is possible to compare the spectrum of complex $\mathbf{2}^-$ with that of $\mathbf{3}^-$; in the latter, bands are observed at 1383 and 1450 cm^{-1}, additional weaker bands being at 1482, 1555, 1602 cm^{-1}.

The spectrum of complex $\mathbf{2}^{2-}$ shows bands at 1597, 1553, 1482 cm^{-1} with 457 nm excitation. At 514 nm bands are observed at 1315, 1482, 1553 and 1597 cm^{-1}. Also observed are features at 1464, 1534 and 1578 cm^{-1}. The first group of bands are assigned as bpy bands. The observation of them at lower frequencies than for $\mathbf{2}^-$ is consistent with the addition of a second electron to the dbn ligand which would be expected to increase the electron density at the metal. The second group of bands are presumably dbn^{2-} features.

Conclusion

This study has demonstrated that the first and second reductions for complexes **1**–**3** are based on the bn or dbn ligand. The resonance Raman spectra of the reduced products confirm the assignment of the first reduction to bn$^{\cdot -}$ or dbn$^{\cdot -}$ formation. It was also possible to observe the spectrum of $\mathbf{2}^{2-}$. This clearly shows a Raman signature unlike that of bpy$^{\cdot -}$ and supports the electronic spectral evidence for the second reduction being at the dbn unit.

Acknowledgements

Support from the New Zealand Lottery Commission and the University of Otago Research Committee for the purchase of the Raman spectrometer is gratefully acknowledged. Support from the University of Otago Division of Sciences for chemicals is also acknowledged. We also thank the University of Otago for the award of a Ph.D. scholarship to S. M. S. and the Massey University Research Fund for funding toward low-temperature crystallographic data collection. This work was funded, in part, by the New Zealand Public Good Science Fund (Contract UOO-508).

References

1 A. von Zelewsky and G. Gremaud, *Helv. Chim. Acta*, 1988, **71**, 1108.
2 S. A. Moya, R. Schmidt, R. Pastene, R. Sartori, U. Muller and G. Frenzen, *Organometallics*, 1996, **15**, 3463.
3 R. P. Thummel, F. Lefoulon, D. Cantu and R. Mahadevan, *J. Org. Chem.*, 1984, **49**, 2209.
4 V. E. Uhlemann, P. H. Thomas and G. Kempter, *Z. Anorg. Allg. Chem.*, 1965, **341**, 11.
5 T. Togano, N. Nagao, H. Kumakura, K. Hisamatsu, F. S. Howell and M. Mukaida, *Inorg. Chim. Acta*, 1992, **195**, 221.
6 C. H. Braunstein, A. D. Baker, T. C. Strekas and H. D. Gafney, *Inorg. Chem.*, 1984, **23**, 857.
7 T. J. Simpson and K. C. Gordon, *Inorg. Chem.*, 1995, **34**, 6323.
8 J. R. Ferraro and K. Nakamoto, *Introductory Raman Spectroscopy*, Academic Press, San Diego, 1994.
9 A. Babaei, P. A. Connor, A. J. McQuillan and S. Umapathy, *J. Chem. Educ.*, 1997, **74**, 1200.
10 D. Pletcher, *A First Course in Electrode Processes*, Alresford Press Ltd., Alresford, 1991, p. 180.
11 M. R. Waterland, T. J. Simpson, K. C. Gordon and A. K. Burrell, *J. Chem. Soc.*, *Dalton Trans.*, 1998, 185.
12 SDP, Structure Determination Package, Enraf-Nonius, Delft, 1985.
13 G. M. Sheldrick, SHELXL 95, Universität Göttingen, 1993.
14 C. K. Johnson, ORTEP, Report, ORNL-5138, Oak Ridge National Laboratory, Oak Ridge, TN, 1976.
15 S. M. Scott, K. C. Gordon and A. K. Burrell, *J. Chem. Soc.*, *Dalton Trans.*, 1998, 2873.
16 R. J. Charlton, C. M. Harris, H. Patil and N. C. Stephenson, *Inorg. Nucl. Chem. Lett.*, 1966, **2**, 409; R. J. Butcher and E. Sinn, *Inorg. Chem.*, 1977, **16**, 2334; K. Folting and L. L. Merritt, jun., *Acta Crystallogr.*, *Sect. B*, 1977, **33**, 3540; A. Parlow and H. Hartl, *Acta Crystallogr.*, *Sect. B*, 1979, **35**, 1930; G. Dessy, V. Fares, P. Imperatori and G. O. Morpurgo, *J. Chem. Soc.*, *Dalton Trans.*, 1985, 1285; W. K. Reagan and L. J. Radonovich, *J. Am. Chem. Soc.*, 1989, **111**, 3881; A. Albinati, C. Ammann, P. S. Pregosin and H. Ruegger, *Organometallics*, 1990, **9**, 1826; R. J. Butcher and E. Sinn, *Inorg. Chem.*, 1977, **16**, 2334; A. L. Spek, A. Gerli and J. Reedijk, *Acta Crystallogr.*, *Sect. C*, 1994, **50**, 394; K. Halvorsen, G. A. Crosby and W. F. Wacholtz, *Inorg. Chim. Acta*, 1995, **228**, 81; R. Bhattacharyya, R. S. Drago and K. A. Abboud, *Inorg. Chem.*, 1997, **36**, 2913.
17 (*a*) M. Draux, I. Bernal, F. Lefoulon and R. Thummel, *Inorg. Chim. Acta*, 1985, **104**, 203; (*b*) S. M. Scott, K. C. Gordon and A. K. Burrell, *Inorg. Chem.*, 1996, **35**, 2452; (*c*) E. Pérez-Cordero, N. Brady, L. Echegoyen, R. Thummel, C.-Y. Hung and S. G. Bott, *Chem. Eur. J.*, 1996, **2**, 781; (*d*) S. M. Scott, Ph.D. Thesis, University of Otago, 1997.
18 R. P. Thummel and F. Lefoulon, *Inorg. Chem.*, 1987, **26**, 675.
19 G. A. Heath, L. J. Yellowlees and P. S. Braterman, *Chem. Phys. Lett.*, 1982, **92**, 646; S. M. Angel, M. K. DeArmond, R. J. Donohoe, K. W. Hanck and D. W. Wertz, *J. Am. Chem. Soc.*, 1984, **106**, 3688; D. E. Morris, K. W. Hanck and M. K. DeArmond, *J. Am. Chem. Soc.*, 1983, **105**, 3032; M. K. DeArmond and C. M. Carlin, *Coord. Chem. Rev.*, 1983, **36**, 325; A. A. Vlcek, *Coord. Chem. Rev.*, 1982, **43**, 39.
20 J. Sherborne, S. M. Scott and K. C. Gordon, *Inorg. Chim. Acta*, 1997, **260**, 199.
21 R. J. Donohoe, C. D. Tait, M. K. DeArmond and D. W. Wertz, *Spectrochim. Acta*, *Part A*, 1986, **42**, 233.
22 P. G. Bradley, N. Kress, B. A. Hornberger, R. F. Dallinger and W. H. Woodruff, *J. Am. Chem. Soc.*, 1981, **103**, 7441.
23 L. De Cola and F. Barigelletti, *Inorg. Chim. Acta*, 1989, **159**, 169.
24 J. R. Schoonover, G. F. Strousse, R. B. Dyer, W. D. Bates and T. J. Meyer, *Inorg. Chem.*, 1996, **35**, 273; M. W. George, F. P. A. Johnson, J. J. Turner and J. R. Westwell, *J. Chem. Soc.*, *Dalton Trans.*, 1995, 2711; L. C. Abbott, C. J. Arnold, T.-Q. Ye, K. C. Gordon, R. N. Perutz, R. E. Hester and J. N. Moore, *J. Phys. Chem. A*, 1998, **102**, 1252.

Paper 8/06443A